THE ASTROPHYSICAL JOURNAL, 422:293–303, 1994 February 10

RADIO CONSTRAINTS ON CORONAL MODELS FOR dMe STARS

S. M. WHITE,[1] J. LIM,[1,2] AND M. R. KUNDU[1]
Received 1992 December 28; accepted 1993 August 20

ABSTRACT

Radio data are used to test coronal models for dMe stars. Specifically, we show that pnotospheric magnetic field observations imply that the low corona of a dMe star should be saturated by magnetic fields with an average strength in excess of 1 kG. In such fields the hot component of the corona detected in X-ray observations (temperature of order 2×10^7 K) would be optically thick at least up to 15 GHz due to thermal gyroresonance opacity. The resulting emission would easily be detectable by radio observations and should have a radio spectrum rising in the microwave range. We have carried out observations to test this prediction, and in the majority of cases find that the observed fluxes at 15 GHz are too low to be consistent with the assumptions. In the few cases where the stars were detected at 15 GHz, the evidence indicates that the observed emission is nonthermal. These results imply that the hot component of the X-ray–emitting plasma in the corona is not coincident with the strong magnetic fields in the lower corona. Because the hot plasma must still be confined by closed magnetic field lines, it is likely to be restricted to heights of the order of a stellar radius above the photosphere. The results seem to imply a different genesis for the two components of the X-ray–emitting corona of flare stars: the hot component may be cooling flare plasma, while the cooler component (temperature of order 3×10^6 K) is associated with a more conventional coronal heating mechanism.

Subject headings: radio continuum: stars — stars: coronae — stars: late-type — stars: magnetic fields

1. INTRODUCTION

The coronae of active stars other than the Sun can now be studied in soft X-rays, EUV, and radio, but are spatially unresolved in all these wavelength ranges. Information on the spatial distribution of matter and magnetic fields in these coronae can therefore only be inferred by indirect means, and for this reason our models of stellar coronae remain somewhat simple. In this paper we take such a simple model for the coronae of dMe stars, inferred from magnetic field and X-ray observations, and show that it suggests a straightforward test using radio data. We have taken appropriate radio observations and collect them together with other data, both published and previously unpublished, and compare them with the predictions of the model. We find that the hot X-ray–emitting component of dMe-star coronae cannot be cospatial with the strong magnetic fields inferred to cover the whole of the lower corona.

2. THE STRUCTURE OF dMe STAR CORONAE: EXISTING EVIDENCE

In this section we will review our knowledge of dMe coronae as deduced from X-ray and photospheric magnetic field observations. The evidence presented here will then be used in the following section to develop a simple model for the corona of a dMe star, which we then show can be used to test the distribution of hot material in the corona with respect to strong magnetic fields.

2.1. *Emission Measure Distributions*

X-ray observations of stellar coronae carried out with spectral resolution can be used to estimate the distribution of plasma in the corona as a function of temperature. The number of free parameters which may be fitted depends on the quality of the data, particularly the spectral resolution, and is model-dependent since the emission measure distribution must be convolved with models for the radiative emission of a plasma of an assumed abundance. When a small number of broad-band filters provides the spectral resolution the number of free parameters which can be plausibly fitted is necessarily small and highly model dependent.

The important outcome of the large number of X-ray observations of dMe stars is that they seem to imply the presence of two components in the coronae: one slightly hotter than a typical solar coronal temperature, and the other an order of magnitude hotter. Most of the early determinations were single-temperature fits (i.e., two free parameters: a temperature and an emission measure corresponding to a single-temperature source) based on *Einstein* IPC observations (Golub 1983). Few M dwarfs were deemed to be bright enough to be worthy of observations with the Solid State Spectrometer (SSS) on *Einstein*: Swank & Johnson (1982) report that both Wolf 630AB and AD Leo have SSS spectra which indicate the presence of components at 7×10^6 K and 4×10^7 K. Pallavicini et al. (1988) discuss the results of broad-band spectroscopy with the *EXOSAT* Low-Energy (LE) detector: they also find results consistent with the presence of material at temperatures in excess of 10^7 K in M dwarf coronae.

The most extensive analysis of the thermal distribution of material in M dwarf coronae has been carried out by Schmitt et al. (1990) using the *Einstein* IPC database. They determined whether the spectra of a wide range of late-type stars were best fitted by a one-temperature (two free parameters), a two-temperature (four free parameters) or a continuous (power law; 3 free parameters) emission measure distribution. Virtually all M dwarfs observed with sufficient signal-to-noise were found to be best described by two-temperature models; by contrast, main-sequence F and G stars required only a single cool thermal component, and RS CVn's often required continuous emission measure distributions extending up to very high temperatures.

[1] Department of Astronomy, University of Maryland, College Park, MD 20742.
[2] Solar Astronomy 264-33, Caltech, Pasadena, CA 91125.

Thus the main result we use here is taken from Schmitt et al. (1990): active M dwarfs typically contain a cool component in their coronae at 3×10^6 K with an emission measure (EM) of $0.5–4 \times 10^{49}$ cm^{-3}, and a hot component at 2×10^7 K with an emission measure of $2–6 \times 10^{49}$ cm^{-3}. Usually the hot component has a larger emission measure than the cool component and provides the larger fraction of the observed *Einstein* 0.2–4 keV IPC X-ray flux. Furthermore, the parameters of the hot component seem to be reasonably stable with time on a timescale of years (Cheng & Pallavicini 1992). For example, there are three separate *Einstein* IPC observations of UV Ceti for which Schmitt et al. (1990) find satisfactory two-temperature fits. They give results of log $T = 7.35^{+0.44}_{-0.18}$, $7.20^{+0.35}_{-0.14}$, and $7.25^{+0.17}_{-0.09}$, with EM = 1.5, 1.7, and 2.6×10^{49} cm^{-3}, respectively; four separate observations of YZ CMi yield log $T = 7.20^{+0.05}_{-0.04}$, $7.40^{+0.22}_{-0.10}$, $7.20^{+0.04}_{-0.14}$, and $7.20^{+0.03}_{-0.08}$, with EM = 6.1, 5.1, 2.34, and 5.0×10^{49} cm^{-3}, respectively. Given the uncertainties, it seems that the temperature and emission measure vary by less than a factor of 2 on the timescale of the *Einstein* mission (2 years). Pallavicini, Tagliaferri, & Stella (1990b) report that during the 3 year lifetime of the *EXOSAT* mission none of the frequently observed dMe's showed variation by more than a factor of 2 in their quiescent level, and the similarity of *Einstein* and *EXOSAT* results (Schmitt et al. 1987) argues against large variations on longer timescales. A possible counterexample is presented by Pollock, Tagliaferri, & Pallavicini (1991), who determined that one of the components of Gliese 867 varied by a factor of 3.5 in X-ray luminosity in the 4 years between *Einstein* and *EXOSAT* observations.

2.2. *X-Ray Observations of Eclipses*

A single measurement of the X-ray spectrum tells us nothing of the spatial distribution of the two components in the stellar atmosphere, which is what interests us here. The only way of doing so presently with X-ray observations is to observe eclipsing systems: knowing the geometry of the eclipse allows timing information to be interpreted as spatial information. This technique requires strong sources so that good spectra can be obtained during the finite eclipse time, and has been successfully applied to RS CVn systems (Walter, Gibson, & Basri 1983; White et al. 1986, 1987, 1990; Culhane et al. 1990; Bedford et al. 1990), many of which are short-period eclipsing binaries. The main limitation to this technique is the problem of secular variability due to flares, which must be separated from variability due to geometrical occultation.

The observations of eclipsing RS CVn's have found that the cool coronal component in those systems may suffer an eclipse, but that the hot component apparently does not (White et al. 1986, 1990; Culhane et al. 1990; however, *ROSAT* observations of AR Lac in Ottman, Schmitt, & Kürster 1993 did find an eclipse of the hot component). This implies that the hot component in the corona of an RS CVn is spatially distinct from the cool component.

There are fewer M dwarf binaries known to be eclipsing. The most suitable is YY Geminorum, consisting of identical dM1e stars in a 19.5 hr eclipsing orbit. *EXOSAT* LE observations of this system, sensitive to the cooler coronal component, were discussed by Haisch et al. (1990). The LE data they present are consistent with a 50% drop in the X-ray flux during the eclipse, which would imply that the bulk of the low-energy X-ray emission arises in relatively low-lying loops close to the stellar surface. Since we are interested in whether both coronal components were eclipsed, and there is no discussion of the Medium Energy experiment data (ME, sensitive in the energy range 1–10 keV) in this paper, even though Pallavicini et al. (1990b) note that YY Gem is one of the few M dwarfs to show quiescent emission in the ME detector, we have investigated the *EXOSAT* data for YY Gem using the data archive maintained by the High Energy Astrophysics group at NASA/Goddard Space Flight Center and present all the eclipse data here for completeness. Note that the data available in the Goddard archive do not separate the contributions of YY Gem and its nearby companion, the Castor system. We have therefore subtracted the fluxes for Castor determined by Pallavicini et al. (1990a) for each scan, and checked that the resulting data are consistent with the mean fluxes for each scan of YY Gem derived by Pallavicini et al. (1990b). Three LE filters were used in these observations: the thin Lexan (3Lex), which is the most sensitive; the parylene–N + aluminium (Al/Pa) combination, primarily sensitive to the cooler coronal component; and the boron, which is mostly sensitive to the hotter coronal component (Pallavicini et al. 1988). Except during a major flare, Castor's flux is significant only in data taken through the 3Lex filter. In Figure 1 we show 4 hours of data centered on each of the four eclipses observed with the LE detector and various filters. The second eclipse on 1984 November 14 (the only one observed at phase 0.5) was interrupted by several filter changes and in Figure 1 we have combined the data from the different filters with the Al/Pa and boron filter data scaled up to match the 3Lex data; a fifth eclipse (on 1984 November 15) has no useful LE data due to filter changes. The eclipse discussed by Haisch et al. (1990) is the one observed with the Al/Pa filter on 1984 February 25.[3] Taken as a whole, it is our impression that these data neither support nor disprove the possibility that the eclipse is seen in the LE data, and therefore there is little evidence on the height distribution of the X-ray–emitting material.

Five eclipses occurred during *EXOSAT* ME observations, and they are shown in Figure 2. The ME data have no spatial resolution, but Castor does not contribute at the higher energies except during a flare (Pallavicini et al. 1990a), and all the flux present can be attributed to YY Gem. The ME data are generally dominated by flares, and several may be seen in Figure 2; in particular, the eclipse on 1984 April 7 occurs at the end of the decay of a significant flare. None of the ME light curves show any evidence for a significant drop in flux at eclipse. However, since we are unable to separate the flaring component from the quiescent component in the ME data, we cannot argue that there is no eclipse in the quiescent ME emission from the hotter coronal component.

2.3. *Photospheric Magnetic Field Observations*

Recent years have been considerable progress in our knowledge of the magnetic fields on M dwarf stars. Early attempts to detect polarization of starlight by the Zeeman effect were unsuccessful, implying upper limits of the order of 100 G on any net dipolar component in late-type dwarfs (Vogt 1980). However, improved versions of the Robinson (1980) technique of comparing magnetically broadened lines of different Landé g factors have proven more successful (Saar 1988). These allow

[3] Note that in their discussion of the eclipse, and in the caption to their Fig. 6*a*, the data are described as taken on 1984 April 7, when a boron filter was used. By comparison with our data we believe that their Fig. 6a does show the light curve for the eclipse on 1984 February 25 seen through the Al/Pa filter, as promised earlier in their paper.

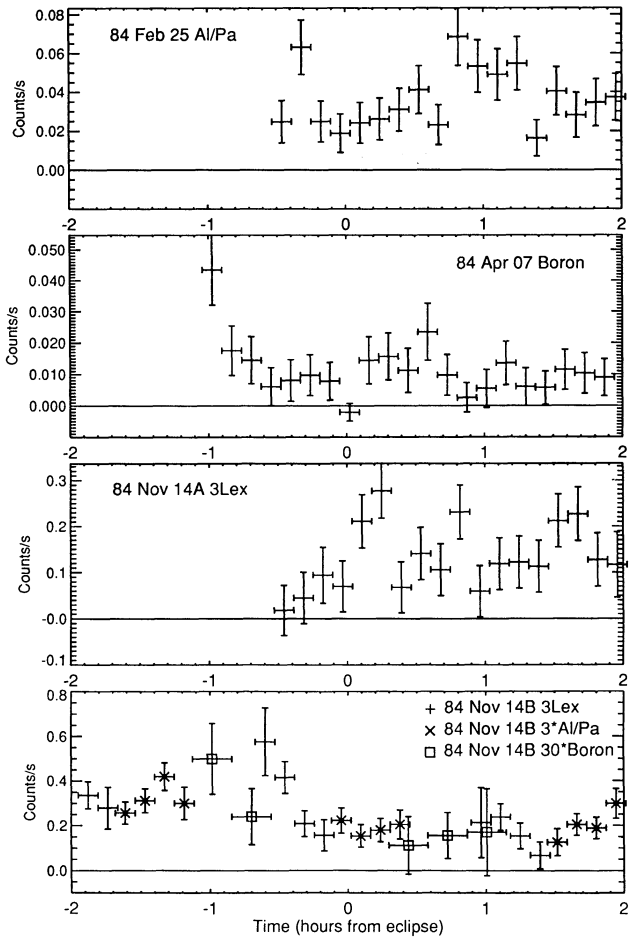

FIG. 1.—*EXOSAT* LE data during 4 eclipses of the YY Gem system. Data are shown for 2 hr on either side of the eclipse, which is thought to be ~2 hr in duration (first to fourth contact). The ephemeris derived by Haisch et al. (1990) was used to determine eclipse times. The top panel is for the eclipse at 6.149 UT on 1984 February 25, seen through the Al/Pa filter; the second panel is for the eclipse at 14.374 UT on 1984 April 7 with the boron filter, the third panel shows the 3Lex filter data for the eclipse at 6.466 UT on 1984 November 14; and the bottom panel shows the eclipse at 16.237 on 1984 November 14 (at phase 0.5) seen through all three filters. The 3Lex filter is much more sensitive than the Al/Pa or boron filters, and in the bottom panel we have scaled the Al/Pa data by a factor of 3 and the boron data by a factor of 30 to display them on the same plot. Error bars are at $\pm\sigma$; the contribution of Castor has been subtracted. All data are binned to 512 s time resolution; there is some artificial overlap of the time intervals for the different filters in the bottom panel.

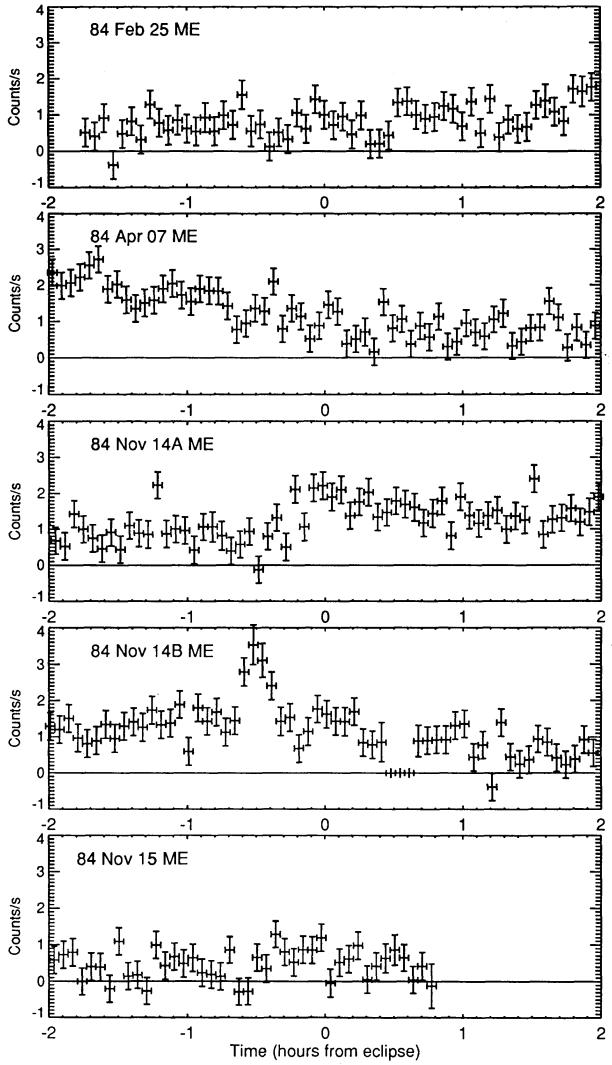

FIG. 2.—*EXOSAT* ME data during 5 eclipses of the YY Gem system. Data are shown for 2 hr on either side of the eclipse. The first four panels correspond to the eclipses shown in Fig. 1; the 5th panel is an eclipse at 2.008 UT on 1984 November 15. Data are binned to 240 s time resolution.

both a magnetic field strength B and an area filling factor f for magnetic fields in the light-emitting regions of the photosphere (i.e., excluding starspots) to be derived.

The results of these observations consistently imply magnetic fields of order 4 kG with filling factors of over 50% on active M dwarf stars (Saar 1990), i.e., much larger filling factors than are found on the Sun even at the peak of the solar activity cycle. Repeated observations seem to show little variation in the derived parameters over a timescale of years, and the use of different lines gives more or less consistent results for the same star (e.g., Saar 1992). As one goes to earlier-type stars the product fB gets smaller. These observations have been critically reviewed by Solanki (1992).

Some work has been done on the distribution of features on the surfaces of stars using light-curve analysis and Doppler-imaging techniques. Light-curve analyses tend to show large polar spots with a relatively small spot area at equatorial latitudes. The existence of such spots would be consistent with theoretical ideas on the rising of magnetic flux to the stellar surface: the Coriolis force tends to drive rising flux tubes toward the poles, and for rapid rotators (as most of the active M dwarfs seem to be) it is actually difficult to see how any flux can reach equatorial laatitudes (Choudhuri & Gilman 1987; Schüssler & Solanki 1992). However, light-curve analyses are known to favor solutions which contain polar spots and the results require confirmation by other techniques (Byrne 1992). Several groups have begun to combine the Doppler and Zeeman techniques by measuring the Stokes parameters for magnetically sensitive lines on stars with large $v \sin i$ (Donati et al. 1990, 1992a; Saar, Piskunov, & Tuominen 1992; Donati, Semel, & Rees 1992b, c). Doppler techniques require bright stars with large $v \sin i$, and thus little information for M dwarfs has been gained so far by this means. In any case, the existence of large spots and the large filling factor of strong magnetic fields in the light-emitting regions of dMes imply that very

strong magnetic fields must cover much of the surface of active M dwarf flare stars.

2.4. *Saturation of Activity Indicators*

The surface X-ray luminosity of flare stars, averaged over the entire stellar surface, is comparable to the surface X-ray luminosity of solar active regions. This, together with the observation that the quiescent X-ray emission does not display obvious rotational modulation or variability on longer timescales (Pallavicini et al. 1990b), suggests that much of the stellar surface is covered by X-ray loops. Indeed, the most active flare stars, apparently irrespective of stellar class in the range dM0–dM6, appear to have the same ratio of quiescent X-ray luminosity to bolometric luminosity: 10^{-3} (Rucinski 1985; Agrawal, Rao, & Sreekantan 1986; Fleming, Gioia, & Maccacaro 1989; Pallavicini et al. 1990b). As pointed out by Pallavicini et al. (1990b) and Pallavicini (1992), the simplest explanation for this dependence is that the entire surface of flare stars is covered by X-ray loops with the same average X-ray brightness per unit area for all stars. Consequently, the stellar X-ray luminosity is simply proportional to the stellar surface area and therefore, given the small range of spectral class indicated, to the bolometric luminosity. (Note, however, that the division of the X-ray–emitting plasma into two components is ignored in this picture.) Stepień (1988, 1991) also uses an indirect argument to estimate the fraction of the corona heated by Alfvén waves and finds that this fraction $f_X \propto f^2$, which would imply that the stars with the largest fraction of surface coverage of strong fields also have the most vigorous coronal heating.

In this view, all activity parameters are related to stellar rotation, which drives the dynamo responsible for stellar magnetic activity. The well-known dependence of activity indicators on rotation reflects the increase in the fraction of the stellar surface covered by active regions (filling factor) with rotation, and saturation occurs when the filling factor reaches 100% (or some threshold value close to 100%). Doyle (1987) attributed the observed saturation of the ratio of the luminosity in the chromospheric Mg II line to bolometric luminosity in rapidly rotating stars to this filling factor effect. There is a similar saturation in the time-averaged U-band luminosity due to stellar flares, at $10^{-4}\ L_{bol}$ (Pettersen 1991).

3. THE CORONAE OF dMe STARS: A SIMPLE MODEL WITH A TESTABLE PREDICTION

In this section we use the information summarized in the preceding discussion to develop a very simple model for the corona of a dMe star, which can then be tested. The main issues in building such a model are (1) what is the coronal magnetic field distribution; and (2) how is the X-ray–emitting material distributed?

3.1. *Coronal Magnetic Field Strength*

The presence of strong magnetic fields over at least 50% of the stellar surface will make the distribution of magnetic fields in the corona of an M dwarf quite different from the example of the Sun. On the Sun the average coronal field strength is very low because the fractional surface coverage of strong fields is very small (a few percent at most). As the surface fields from active regions rise up into the low-pressure corona, the magnetic energy density far exceeds the local thermal energy density and the magnetic pressure causes the magnetic flux tubes to expand rapidly out over regions of the solar surface where the magnetic field is low (e.g., Zwaan & Cram 1989). As they expand the field strength drops rapidly by flux conservation. The net result is that the fraction of the solar corona in which the magnetic field exceeds 1 kG is tiny.

However, on M dwarf stars any given parcel of magnetic flux will not expand rapidly as a function of height in the corona, because the surface coverage of strong magnetic fields is so high that the magnetic flux cannot expand far without running into a neighboring region of strong magnetic field which prevents further expansion. The actual dependence of field strength with height will depend on the magnetic field topology: specifically, how much of the magnetic flux is associated with open field lines (small on the Sun), how much of the flux returns to the surface very close to where it emerges, and how much returns to the surface far from where it emerges. If most of the flux associated with closed field lines returns to the surface close to its emergent point, corresponding to a photospheric magnetic pattern consisting of many small spots of mixed polarity, then the effective magnetic scale height will be small. If, on the other hand, most of the positive flux is at one pole and the negative flux is at the other, the scale height will be large (although the lack of circular polarization in Zeeman measurements seems to contradict such a model; Vogt 1980). One can also think of the magnetic field distribution in terms of the multipole components of the field distribution: a complex surface field distribution corresponds to having strong high-order components, whereas a large-scale global field corresponds to the dominance of the lowest order (dipole) component.

Whether the scale height is large or small, it is clear that in the low corona the mean magnetic field strength must be high because of the limitation on flux tube expansion. If we assume that the photospheric flux expands to fill the entire surface of the low corona, we can use fB as a rough estimate of the mean field strength in the low corona: this has the value 2.3 kG for AU Mic (dM1.5e), 2.6 kG for AD Leo (dM3.5e), and 3.6 kG for EV Lac (dM4.5e) (Saar 1993).

On the Sun, regions of high magnetic field strength in the corona appear bright in radio observations due to the fact that gyroresonance opacity makes these regions optically thick. However, the area which is optically thick at frequencies above 10 GHz is negligible. Since gyroresonance opacity increases with temperature, active stars which have coronae hotter than the Sun's should produce relatively more gyroresonance emission at higher frequencies. Let us assume that the hotter component of X-ray corona is uniformly distributed in the stellar corona and occurs low enough in the corona to experience kilogauss magnetic fields. We assume nothing about the cooler component of the X-ray corona for the moment. In the remainder of this section we will investigate whether the hot component can be detected through high-frequency radio observations. The reasons for choosing high frequencies are twofold: (1) the flux of an optically thick thermal source increases with frequency; and (2) the problem of discriminating against nonthermal emission, which is known to dominate emission at 1.5 GHz, is lessened, since the nonthermal emission is expected to be optically thin at high frequencies and thus should have a flux spectrum falling with frequency. We therefore investigate the properties of the coronae at 8 and 15 GHz, the two frequencies at which the Very Large Array operates which are most convenient for such a study.

3.2. *Density and Distribution of the Hot X-Ray–emitting Component*

We now investigate whether the hot component is likely to be optically thick in the corona of a typical dMe star at radio wavelengths. We must first estimate the number density for the hot X-ray–emitting component. The gravitational scale height would be many stellar radii, and it is widely believed that this component is confined by strong magnetic fields. The effective scale height for the hot coronal material is therefore the scale height of the coronal magnetic field: we assume that the hot component occupies a shell surrounding the star of depth approximately equal to the magnetic scale height in the stellar corona, L_B. In that case the mean number density is approximately related to the emission measure as follows:

$$n = 7 \times 10^7 \text{ cm}^{-3} \left(\frac{R_*}{R_\odot}\right)^{-1.5} \left(\frac{L_B}{R_*}\right)^{-0.5} \left(\frac{\text{EM}}{10^{49} \text{ cm}^{-3}}\right)^{0.5} . \quad (1)$$

Note that in deriving this formula we have assumed that $L_B < R_*$ and we have ignored small corrections of the kind discussed by Katsova, Badalyan, & Livshits (1987). This formula is only expected to be accurate to a factor of order 2, which is adequate for our purposes.

3.3. *Optical Depth and Flux at Radio Wavelengths*

The optical depth of this material at a frequency F and harmonic number s is

$$\tau(s,f) = \frac{\pi^3}{4} \frac{f_p^2 L_B}{Fc} \frac{s^2(2s-2)!}{2^{2s-2}s![(s-1!)]^2} \left(\frac{s^2}{2\mu}\right)^{s-1}$$

$$= 1.45 \frac{L_B}{R_*} \frac{R_*}{R_\odot} \frac{n}{F_{\text{GHz}}} \begin{cases} 1.3 \times 10^{-4} \left(\dfrac{T}{2 \times 10^7 \text{ K}}\right)^2, & s = 3; \\ 4.1 \times 10^{-6} \left(\dfrac{T}{2 \times 10^7 \text{ K}}\right)^3, & s = 4; \\ 1.8 \times 10^{-7} \left(\dfrac{T}{2 \times 10^7 \text{ K}}\right)^4, & s = 5; \end{cases} \quad (2)$$

where f_p is the local plasma frequency, and $\mu = mc^2/kT$. Here we have averaged the expression given by White, Kundu, & Gopalswamy (1992) over angle and polarization. Gyroresonance opacity is a sharp function of viewing angle, particularly as one goes to higher harmonics, and the average over angle approximately accounts for this. Equations (1) and (2) may be combined to calculate an opacity at a given frequency for a given harmonic (or equivalently, a given magnetic field since $F_{\text{GHz}} = 2.8 \times 10^{-3} sB$).

We do not know in advance the magnetic scale height, but fortunately the opacity depends only weakly on it: $\tau \propto L_B^{0.5}$, so that the larger the scale height, the larger the opacity. To calculate several examples, we will adopt a magnetic scale height of 0.3 stellar radii. If the scale height is any smaller than this, we would expect that eclipse observations should show deep eclipses of the hot X-ray–emitting component. For UV Ceti AB the parameters from Schmitt et al. (1990) are $T = 2.2 \times 10^7$ K and EM $= 0.8 \times 10^{49}$ cm^{-3} (dividing the observed flux equally between the two components); with $R_* = 0.14\ R_\odot$ we find a density $n = 2.2 \times 10^9$ cm^{-3}, corresponding to an energy density of $nkT = 7$ ergs cm^{-3}. At 15 GHz this provides an optical depth of 2.4 for the 5th harmonic ($B = 1070$ G) and 49 for the 4th harmonic ($B = 1330$ G); at 8 GHz the optical depth would be 4.4 at the 5th harmonic ($B = 570$ G) and 93 at the 4th harmonic ($B = 710$ G). For YY Gem AB, where $T = 2.8 \times 10^7$ K and EM $= 3.8 \times 10^{49}$ cm^{-3} (again dividing the observed flux equally between the two components) with $R_* = 0.6\ R_\odot$, the implied density is $n = 5 \times 10^8$ cm^{-3}. At 15 GHz this provides an optical depth of 6 for the 5th harmonic and 97 for the 4th harmonic; at 8 GHz the optical depth would be 11 at the 5th harmonic and 190 at the 4th harmonic. Thus under likely conditions only a coronal field of 1070 G (i.e., much smaller than the measured values of fB) would be required to make the coronae of these stars optically thick at 15 GHz; note that the energy density of the thermal component is much smaller than the magnetic energy density ($\sim 4 \times 10^4$ ergs cm^{-3} in a 1 kG field). The effect of our choice of magnetic scale height may now be estimated from the derived opacities: since $\tau \propto L_B^{0.5}$, and we find $\tau \gg 1$ for most cases, the scale height would need to be very small (the assumed scale height divided by the optical depth, or of order $0.01\ R_*$) to avoid having the corona optically thick.

The radio flux we predict from a star under the assumption of an optically thick source is then

$$S = 2.24 \text{ mJy} \frac{T}{2 \times 10^7 \text{ K}} \left(\frac{F}{15 \text{ GHz}}\right)^2 \left(\frac{d}{5 \text{ pc}}\right)^{-2} \left(\frac{R}{1/2R_\odot}\right)^2 . \quad (3)$$

Here R is to be regarded as the radius of the radio source: according to this simple model the radio source should be the projected area on which the corona is optically thick. Because of the large filling factor of strong magnetic fields, this should be of order of the stellar radius or larger.

We also note that the Alfvén speed in this coronal model is very high: unless the density exceeds $\sim 10^{10}$ cm^{-3}, the Alfvén speed will exceed the speed of light throughout the corona.

3.4. *Predictions*

Thus a model in which the hot component of the X-ray–emitting plasma is confined to the loops where the magnetic field is strong, together with the implications of the magnetic field measurements for M dwarfs, leads to a prediction which is testable by radio observations: these stars ought to have a quiescent flux at 15 GHz of the order of several mJy, which is easily detectable by the Very Large Array (VLA); the spectrum between 8 and 15 GHz ought to vary as F^2 unless there is a significant nonthermal contribution at 8 GHz; and the flux ought to be stable over long timescales, as the X-ray parameters and mean magnetic field strength are found to be.

The idea that the high-frequency radio emission of dMe stars can be explained by thermal gyroresonance emission is not new. Gary & Linsky (1981) originally proposed this as the explanation of their 5 GHz detection of UV Cet, although at 5 GHz one must always either assume much larger sources ($3R_*$) than we assume here, or else brightness temperatures much higher than the temperature of the hot component observed in X-rays. Gary (1985) gave the arguments that the combination of strong magnetic fields covering a large fraction of the stellar surface together with hot coronae should produce more radio emission than on the Sun. Cox & Gibson (1985) found an instance where the 15 GHz flux of AU Mic exceeded the 5 GHz flux and interpreted the 15 GHz emission as thermal (although they did not specify whether they meant thermal bremsstrahlung or thermal gyroresonance opacity), deriving a temperature of 2×10^7 K in agreement with the X-ray

observations. Gary (1986) used a model consisting of one thermal component at 10^7 K and another at 3×10^8 K to model the flux spectrum of dMe's, assuming a very strong surface field (10 kG) due to a dipole buried at a depth of $0.3R_*$. This model gave an acceptable fit to observations of YY Gem; the spectral peak at 5 GHz in this model fitted observations which found the 15 GHz flux to be much smaller than the 5 GHz flux. The hot component produced the low-frequency emission, and the cooler component produced the high-frequency emission. Güdel & Benz (1989) measured the spectrum of UV Ceti from 0.33 to 22 GHz, and found that the flux was rising from 15 to 22 GHz in accord with a thermal gyroresonance model. They interpreted the observed spectrum as consisting of a nonthermal component dominant at low frequencies, together with thermal gyroresonance emission from a component at a similar temperature to the X-ray–emitting material. They derived numbers for their thermal gyroresonance source which are very similar to those used here.

The difference in the approach adopted here is that we argue that all of these stars should regularly be detected at 15 GHz with an optically thick thermal spectrum if the assumptions discussed above hold true. The basic predictions of the model are that the 8 GHz fluxes should be at least at the level of the predicted flux, since any nonthermal contribution persisting up as high as 8 GHz should add to the thermal flux; if the 8 GHz flux looks to be consistent with the thermal prediction then the 15 GHz flux ought to be ~ 3 times higher (taking into account the fact that the optically thick 15 GHz source will not be as large as the 8 GHz source); and the 15 GHz flux ought to be similar to the predicted value since a field of only 1070 G is required in the corona to achieve this value. The 15 GHz flux ought to be steady with time to be consistent with the X-ray data; it might show some rotational modulation (timescale of days) since it is unlikely that the coronal material is at a uniform temperature. The model does not say anything about polarization of the radio emission, which could be substantial if the source is pole-on and has a large dipolar component, but small if the source is equator-on or has a complex field distribution.

4. HIGH-FREQUENCY MICROWAVE SPECTRUM OF dMe STARS: OBSERVATIONS

4.1. *Data Selection*

While there are some published observations suitable for this kind of study, they are not systematic enough to draw any firm conclusions. We have therefore obtained additional VLA[4] observations of a number of stars well observed in X-rays. In this section we combine these data together with data both previously unpublished and obtained from the literature.

4.2. *New Observations*

The observations were carried out on 1992 May 31. Seven stellar systems (EQ Vir, BY Dra, CC Eri, YY Gem, DT Vir, Gl 867, and EQ Peg) were observed at 8 and 15 GHz; they were chosen from the list of dKe/dMe stars for which two-temperature fits are listed by Schmitt et al. (1990), and are the stars visible during the LST range (23:00–12:00) of the observations. In order to achieve suitable sensitivities at both frequencies, bearing in mind our test of a model in which flux rises as frequency squared, the sources were observed for integration times of ~ 60 minutes at 15 GHz (two 50 MHz sidebands at 14.664 and 15.064 GHz) and 20 minutes at 8 GHz (two 50 MHz sidebands at 8.064 and 8.464 GHz). This resulted in 3 σ detection levels of ~ 0.25 mJy at 15 GHz and 0.12 mJy at 8 GHz. A number of antennas were missing from the array due to the configuration change taking place at the time. Each 15 GHz observation consisted of several scans spread over a range of hour angles; the 8 GHz data were generally taken in a single scan. The maps were cleaned out to the edge of the primary beam.

[4] The Very Large Array is a facility of the National Radio Astronomy Observatory, which is operated by Associated Universities, Inc., under cooperative agreement with the National Science Foundation.

4.3. *Other Data*

The stars observed as part of this program are listed in Table 1, together with a number of properties required to calculate radio fluxes based on the above model. In addition, we have compiled all observations in the literature at the same frequencies and added them to the table. The stars are ordered according to the spectral type given in the latest version of Gliese's catalog of nearby stars. Distances are derived from the same catalog. Stellar radii are those given by Pettersen (1980) where possible, and otherwise are those used by White, Jackson, & Kundu (1989) and derive either from Lacy (1977) or from the relation given by him. We note, however, that there is considerable uncertainty in these radii, as may be seen by comparing the values given by Lacy (1977) with those for the same stars given by Pettersen (1980); in particular, Pettersen's (1980) radii lead to fluxes for EQ Vir and YY Gem which are a factor of ~ 2 lower than would Lacy's (1977) radii. There is considerable variation of radius for stars of the same stellar type, which is usually attributed to age (younger stars are still contracting and hence have larger radii). The table includes predicted flux values at 8 and 15 GHz based on the assumption that the star's corona is optically thick over an area equal to the projected stellar surface with a temperature equal to that of the hot X-ray–emitting component. Where no X-ray temperature determination exists, we have used a "default" value of 2×10^7 K which has been placed in parentheses in the table (see also the notes to Table 1). Magnetic field information is given for those stars which have been measured (Saar 1990, 1993).

We emphasize at the outset that the predicted fluxes at 8 and 15 GHz are only rough estimates, since even if we assume that the X-ray temperatures are well determined there remain large uncertainties in the source size which we assume. However, based on the large filling factors of the strong magnetic fields, we think it reasonable to assume that the projected stellar area is an appropriate lower limit to the size of an optically thick coronal source, but as discussed above it could easily be much larger if the magnetic scale height is large. Thus the numbers given should be suitable as lower limits for comparison with observations.

4.4. *Results*

Four of the seven targets of our new VLA observations were detected at 8 GHz, but only one was detected at 15 GHz. Both components of Gliese 867 were detected at 8 GHz, with Gliese 867A (dM2) the stronger source (0.22 mJy), in contrast to the two previous radio observations (White et al. 1989) in which only Gliese 867B (dM4e) was detected at both 1.5 and 5 GHz. The model predicts that Gliese 867A should have ~ 4 times as much flux as Gliese 867B, but the observed ratio is less than 2. BY Draconis, DT Virginis, and EQ Virginis were undetected at 8 GHz with 3 σ upper limits below the predicted 8 GHz flux.

TABLE 1

PREDICTED AND OBSERVED RADIO FLUXES FROM dMe STARS

Name (1)	Type (2)	Distance (pc) (3)	$R_*/R_\odot$ (4)	EM $\times 10^{49}$ cm^{-3} (5)	log T (6)	fB (kG) (7)	Predicted S_8 (mJy) (8)	Predicted S_{15} (mJy) (9)	Observed S_8 (mJy) (10)	Observed S_{15} (mJy) (11)	Notes (12)
EQ Vir	K5	19.2	0.56	1.39	7.45	2.0	0.08	0.27	<0.11	<0.28	a
									0.12 ± 0.04		b
BY Dra	K6Ve	17.2	0.99	6.76	7.20	1.7	0.17	0.59	<0.09	<0.29	a
CC Eri	K7Ve	11.5	0.81	3.92	8.20	...	2.50	8.81	0.52 ± 0.042	<0.23	a
									3.02 ± 0.03		b
AU Mic	M0Ve	9.4	0.56	37.30	7.30	2.3	0.23	0.79	<0.12	<0.21	c
										1.0 ± 0.1	d
Gl 182	M0.5V	16.4	0.51	...	(7.30)	...	0.06	0.22	...	<1.3	e, f
										3.0–9.0	g
YY Gem AB	M0.5Ve	14.6	0.62	7.21	7.45	...	0.09	0.33	3.86 ± 0.042	1.99 ± 0.09	a, h
										0.3–2.0	i
DT Vir	M1.5Ve	11.1	0.79	1.98	7.20	...	0.26	0.90	<0.13	<0.23	a
Gl 867 AB	M2e	8.7	0.69	9.01	7.30	...	0.40	1.41	0.20 ± 0.027	<0.25	a
	M4e	...	0.35	...	...	...	0.10	0.36	0.13 ± 0.027	<0.25	
Kruger 60A	M2	4.0	0.35	...	(7.30)	...	0.49	1.71	...	<0.48	j, k
DO Cep	M6		0.22	...	...	...	0.19	0.68	...	<0.48	
Gl 890	M2.5e	24.6	0.68	1400	7.21	...	0.04	0.14	0.25 ± 0.08	...	l, m
										1.40 ± 0.46	n
Wolf 630 AB	M3	6.5	0.45	...	(7.30)	...	0.30	1.07	...	1.56 ± 0.11	j, o, p
										1.45 ± 0.47	n
EQ Peg AB	dM4e	6.6	0.39	14.20	7.35	...	0.25	0.88	<0.12	<0.21	a
	dM6e	...	0.23	...	...	...	0.09	0.30	1.0 ± 0.038	<0.21	a, q
AD Leo	M4.5Ve	4.9	0.44	...	(7.30)	2.6	0.51	1.80	...	<0.2	o, r
										5–30	s
YZ CMi	M4.5e	6.2	0.37	5.09	7.40	...	0.28	1.00	...	<1.6	f
L726-8A	M5.5e	2.6	0.14	1.52	7.35	...	0.21	0.73	0.4 ± 0.1	0.55 ± 0.1	t
										<0.3	r
UV Cet	M5.5e	...	0.14	...	...	...	0.21	0.73	1.1 ± 0.1	1.6 ± 0.1	t
									1.6 ± 0.1	1.6 ± 0.1	t
										0.86 ± 0.1	r
Wolf 424 AB	M5.5e	4.3	0.17	...	(7.30)	...	0.10	0.35	...	<0.29	j, k
	M7	...	(0.10)	...	...	...	0.03	0.12	...	<0.29	
Prox Cen	M5e	1.3	0.15	6.97	7.30	...	0.85	2.98	<0.22	...	u

NOTES.—Entries are ordered according to the spectral type (using the primary in the case of binary systems). The systems UV Cet/L726 − 8A (2″), EQ Peg (6″), DO Cep/Krüger 60 A (3″), and Gliese 867 AB (24″) are binaries in which the two components are usually resolvable in high-frequency radio observations; separate entires are given for each star in the Table. Wolf 630 AB (0.2″) and Wolf 424 AB (1″) are close binaries which may not always be resolvable. CC Eri, BY Dra, YY Gem, and Gliese 867 A are all unresolved spectroscopic binaries. Common star names are given in Col. (1). Spectral types (col. [2]) and distances (col. [3]) are taken from the preliminary third revision of the Gliese Catalogue of Nearby Stars. Stellar radii in units of solar radius (col. [4]) are taken from Pettersen 1980 where possible, otherwise from Lacy 1977. The X-ray emission measure and temperature (cols. [4] and [5]) are taken from Schmitt et al. 1990; hot component). Magnetic field data (product of mean field strength and filling factor, col. [7]) are from the review by Saar 1990. The predicted 8 and 15 GHz fluxes (cols. [8] and [9]) are calculated from the temperature, radius and distance as described in the text. The flux measurements (cols. [10] and [11], with ±1 σ uncertainties or 3 σ upper limits) are from sources indicated in the specific Notes (col. [12]) which follow:

[a] Radio observations carried out 1992 May 31 for this paper.

[b] Measurements by Güdel 1992 in 1992 January. All emission was apparently steady; polarization is not mentioned.

[c] Radio observations carried out 1991 September 7 during *HST*/GHRS campaign for AU Mic; *Australia Telescope* observations carried out several hours later also yielded no detection (R. T. Stewart & O. B. Slee, private communication).

[d] Observed by Cox & Gibson 1985 five times during a 14 day period; apparently steady over this time. The emission was unpolarized.

[e] Gliese 182 is thought to be much younger than the other dMe's on this list, with the possible exception of Gliese 890. It was observed three times by the *Einstein* IPC, but only one of the three observations gave a satisfactory two-temperature fit and that is listed as "log $T = -8.25$". We have therefore calculated a radio flux based on a default temperature of 2×10^7 K, which is an order of magnitude too low if the IPC value is appropriate.

[f] Observed by Slee et al. 1988.

[g] A 6 minute observation reported by Mathioudakis et al. 1991 during which Gl 182 appeared variable. The emission was unpolarized; the star was not detected at 5 GHz with an upper limit of 0.4 mJy.

[h] YY Gem was variable but unpolarized at both 8 and 15 GHz during the observation.

[i] Observed by Gary 1985. Source was variable but unpolarized at 15 GHz; the variability is attributed to rotational modulation.

[j] Radio observations carried out 1987 June 18 by P. D. Jackson.

[k] No temperature fit to X-ray data reported, so a temperature of 2×10^7 K assumed.

[l] X-ray data from a single-temperature fit to *EXOSAT* data by Rao & Singh 1990.

[m] Observation by S. M. White on 1991 June 1; marginal detection at 3 σ. Subsequent observations by M. Güdel 1994, have also detected Gl 890 at a slightly higher level at both 8 and 15 GHz.

[n] Also a marginal detection, by Slee et al.

[o] *Einstein* IPC data yielded no satisfactory fit for either a one-temperature, two-temperature, or continuous power-law emission measure fit (Schmitt et al. 1990).

[p] Wolf 630 AB flared during observations, so this 15 GHz flux is not a quiescent component; the emission was unpolarized. Flares at 1.5 and 5 GHz during same observations were negatively polarized. Wolf 630 C was not observed.

[q] EQ Peg B (only the secondary was detected) was highly polarized (in the positive sense) at 8 GHz during the observation, but did not vary significantly during the 7 minute observation.

[r] Observations by S. M. White on 1989 October 4 (UV Cet) and 1990 February 15 (AD Leo). The emission of UV Cet was probably variable.

[s] Detected during a flare program with low sensitivity to quiescent emission by Rodonó et al. 1989. Flare was detected simultaneously at 5 GHz, in the optical U band and the near-infrared K band (as a depression). The flare was not detected at 1.5 GHz. Both the 5 and 15 GHz emissions were unpolarized (D. Gary, private communication).

[t] Observations by Güdel & Benz 1989 on two separate days in 1987 October. All emission was unpolarized; the primary, L726–8A, was only detected on one of the two days. The secondary, UV Ceti, is the more active star.

[u] *Australia Telescope* observation on 1991 August 30; J. Lim, G. Nelson, and S. M. White, 1994.

All these stars were undetected at 15 GHz: the upper limit for EQ Vir is close to the predicted model flux, while for DT Vir and BY Dra the upper limit is a factor of 2–3 below the predicted flux.

EQ Pegasi B (dM6e) was the only star detected at 8 GHz to show any circular polarization: the total intensity was 1.0 mJy with a circularly polarized flux of 0.8 mJy, polarized in the positive sense. Its companion, EQ Peg A (dM4e), was not detected at 8 GHz, and neither was detected at 15 GHz: EQ Peg A was a factor of 4 below its predicted flux, while EQ Peg B's upper limit is about the same as the predicted flux. The high degree of polarization clearly implies a nonthermal emission mechanism at 8 GHz; however, analysis of the visibilities at 2 minute intervals indicates that there is no evidence for significant variations in the flux over the 20 minutes of the observation. This observation contrasts with the observation of EQ Peg by Kundu et al. (1988), in which EQ Peg A was a slowly varying, unpolarized 9 mJy source at 5 GHz over 8 hr while EQ Peg B was undetected; at 1.5 GHz EQ Peg B produced flares polarized in a positive sense. Topka & Marsh (1982) detected both components at 5 GHz at similar fluxes, while Jackson, Kundu, & White (1989) detected only EQ Peg A at 5 GHz.

YY Geminorum was the strongest source detected in these observations at 8 GHz (3.9 mJy), and was the only source detected at 15 GHz (2.0 mJy). It was unpolarized at both frequencies ($<3\%$ at 8 GHz, $<13\%$ at 15 GHz using 3 σ upper limits to the polarized flux) but clearly varied during the observation: Figure 3 presents the time variability at 8 and 15 GHz. A slow rise is seen at 15 GHz, followed by a sharp rise at 8 GHz. It is clear that this emission cannot be attributed to the steady thermal emission predicted by the model. Nearly all previous detections of YY Gem at 5 GHz and higher frequencies have also been unpolarized (Linsky & Gary 1983; Gary 1985; Jackson et al. 1989).

CC Eri is the star with the highest predicted fluxes in Table 1, due to the large X-ray temperature (1.6×10^8 K) given by Schmitt et al. (1990). It was detected at 8 GHz (0.52 mJy) but not at 15 GHz (<0.23 mJy). The emission at 8 GHz was unpolarized and apparently steady on a 2 minute timescale. The implied flux spectrum is not compatible with the thermal model.

4.5. *Summary*

The 8 GHz data show observed fluxes of the correct magnitude for Gl 867A, Gl 867B and L726–8A; they are much larger than predicted for YY Gem, EQ Peg B, Gl 890, and UV Cet; and too small for CC Eri, AU Mic, EQ Peg A, and Prox Cen. In all four cases where the flux is too large, there is reason to think that the 8 GHz flux is mostly nonthermal.

The 15 GHz data provide the strongest test of the model, since the predicted fluxes are larger and we expect that the effects of nonthermal emission will be weaker. Figure 4 shows the observed fluxes plotted against the predicted fluxes for those cases in Table 1 where there is no evidence that the fluxes are nonthermal (see notes). Most of the observations place upper limits on the flux which are well below the predicted levels. In the case of UV Ceti, our predicted flux happens to be within a factor of 2 of the 15 GHz measurement by Güdel & Benz (1989), which supports their interpretation of that measurement as gyroresonance emission; however, most of the 15 GHz data are in conspicuous disagreement with such an interpretation.

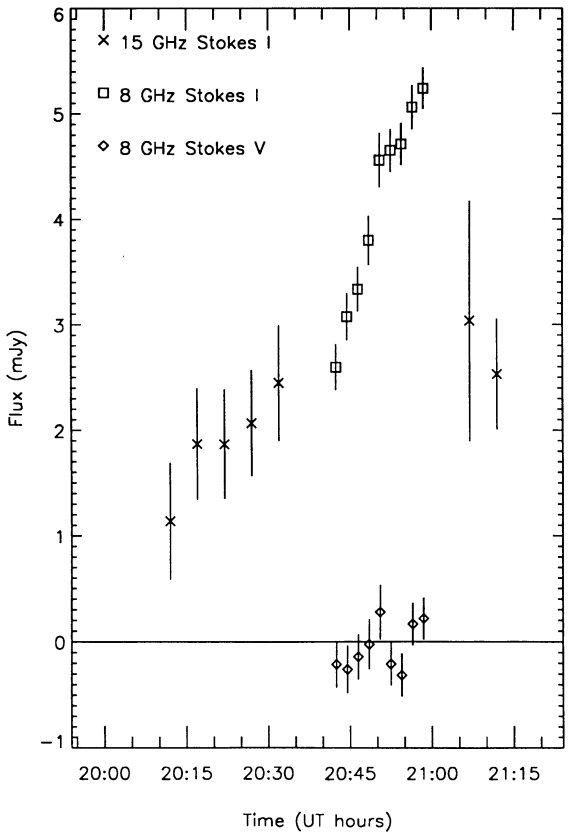

FIG. 3.—The time variation of the Stokes I (total intensity) and Stokes V (circularly polarized) fluxes from YY Gem at 8 and 15 GHz. The time resolution is 4 minutes at 15 GHz (crosses, Stokes I only) and 2 minutes at 8 GHz (*squares*, Stokes I; *diamonds*, Stokes V). Error bars are at $\pm\sigma$.

The fluxes at 8 and 15 GHz are also generally inconsistent with an optically thick thermal spectrum rising as F^2. Unfortunately our observations do not place any strong constraints on the spectrum of the nonthermal emission, since the upper limits at 15 GHz are usually above the detected flux at 8 GHz. The best data for studying the nonthermal spectrum remain those of Güdel & Benz (1989).

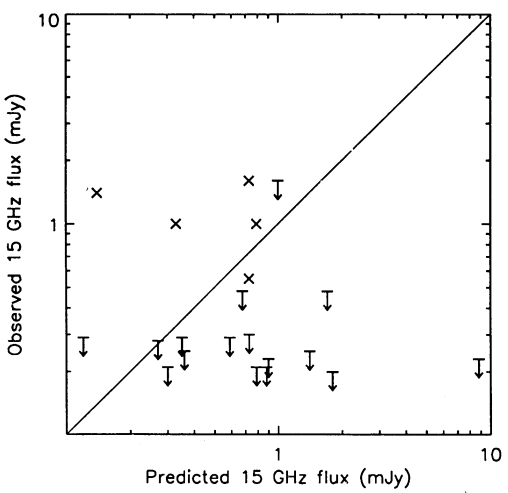

FIG. 4.—Detection levels (*crosses*) and nondetections (3 σ upper limits, *arrows*) at 15 GHz, plotted against the predicted 15 GHz fluxes.

We also note that successive observations of the same star can yield fluxes which differ by a large amount, which (if the radio emission were to arise by the model described here) contradicts the idea that the X-ray corona and the mean magnetic field strength in the lower corona are somewhat stable.

4.6. *Polarization*

One of the interesting results of this compilation of data is the absence of detected circular polarization at 15 GHz. Nine of the stars in Table 1 have been detected at 15 GHz, at levels of up to 30 mJy and with many showing temporal variability, but none have shown any circular polarization. This contrasts greatly with observations at longer wavelengths: at 1.5 and 5 GHz the flares are usually highly polarized (Gary, Linsky, & Dulk 1982; Kundu & Shevgaonkar 1985, 1988; Lang & Willson 1986, 1988; White et al. 1986; Bastian & Bookbinder 1987; Jackson, Kundu, & White 1987, 1989; Kundu et al. 1988; White, Jackson, & Kundu 1989; Bastian et al. 1990). There have been few reported VLA observations at 8 GHz (this frequency was not available at the VLA during the early observations of dMe stars), and of those, so far only the emission of EQ Peg B reported here has been polarized.

4.7. *High-Frequency Flares*

The apparently broad-band flare observed on YY Gem is one of the few examples of its type: most detections of dMe radio flares have been during single-frequency observations, or else the multifrequency observations indicated that an M dwarf flare was narrow band (e.g., see review by Bastian 1990). The implied brightness temperature of the flare is $5 \times 10^8 (R/R_*)^{-2}$ K, and for plausible source sizes R the brightness temperature will be within the usual range of gyrosynchrotron emission. The other good example of a broad-band radio flare detection may be found in Rodonó et al. (1990).

This suggests that we may have to account for three types of radio emission on dMe stars: the coherent, usually highly circularly polarized flares which are seen at low frequencies, the "quiescent" emission, which is probably nonthermal, unpolarized and does not vary on timescales of an hour, and unpolarized broad-band flares seen at higher frequencies, which may well be similar to the nonthermal unpolarized radio flares shown by RS CVn systems.

5. INTERPRETATION

The results of high-frequency observations of dMe stars do not seem to be consistent with the predictions of the simple model outlined earlier. We note that absorption by overlying material (which has been invoked in the context of solar radio emission; see, e.g., Webb et al. 1987 and Nitta et al. 1991) is not a possible explanation for the low 15 GHz fluxes, because of the following argument. At 15 GHz only gyroresonance opacity could provide enough absorption (free-free opacity will be negligible at these high frequencies); the absorbing material would presumably be on average higher in the atmosphere than the hot plasma, and therefore be in a weaker magnetic field. The opacity of plasma cooler than the hot X-ray–emitting component at a higher harmonic for the same observed frequency would necessarily be smaller (by a factor of order $\mu^{-1} \sim 10^{-3}$; see eq. [2]). The low opacity will prevent any significant absorption in overlying cool material.

One possibility is that the photospheric magnetic field measurements are not correctly interpreted. The interpretation of the observations of the magnetically broadened lines continues to be critically tested and explored (e.g., Solanki 1992; Saar 1992, 1993). For example, Saar (1992) showed how different models for the distribution of magnetic field with height led to different results for fB from observations of AD Leo. However, Saar (1993, private communication) reports that the lines on active saturated stars cannot reasonably be modeled without $fB > 2$ kG (with a probable upper limit of 5 kG). Our model requires only $fB = 1.1$ kG if the corona is to be optically thick at 15 GHz at the 5th gyroharmonic, and 1.3 kG for the 4th harmonic, and we reject errors in the interpretation of the magnetic field observations as a possible explanation for our results.

Consequently, some of the assumptions going into our simple model must be incorrect: either the hot plasma is not cospatial with the strong magnetic fields in the lower corona, or the magnetic fields in the corona are not as strong as simple extrapolation of the photospheric results seems to imply.

For the present we discard the latter alternative: unless the chromosphere of the typical dMe star is relatively thick and the horizontal spatial scale of the magnetic fields at the photosphere is very small, it is difficult to see how significant amounts of flux emerging in the photosphere can close in the chromosphere. It would require that the magnetic field be organized in many small concentrations such that the separation of opposite polarities be of the order of the height of the transition region: only then can a significant amount of magnetic flux emerging at the photosphere consist of loops closing underneath the corona. Since the gravity at the surface of an M dwarf is greater than at the solar surface, the gravitational scale height in an M dwarf chromosphere is smaller than on the Sun, and hence there is no reason to assume a thick chromosphere on M dwarf stars (most models assume hydrostatic equilibrium in the chromosphere, e.g., Cram & Giampapa 1987). In that case, a magnetic field distribution of many oppositely polarized features several thousand kilometer apart seems to be inconsistent with the observations of large photometric modulations which are attributed to large spots. Montesinos & Jordan (1993) use indirect scaling arguments to estimate the mean coronal field strength, using in particular the assumption that B^2 (in the corona) is proportional to coronal pressure, and find that the coronal field is $\propto (fB)^{0.4}$ (with fB measured in the photosphere). This would imply that not all the photospheric magnetic flux does reach corona, but it is not clear how to relate their indirect arguments to our specific model.

Consequently we must conclude that the hot coronal plasma is not coincident with the strong magnetic fields. There are several ways in which this might occur.

1. The strong magnetic fields are confined to magnetic flux tubes which do not expand in the corona, leaving lower field regions between them which can be occupied by the hot X-ray–emitting plasma. The cool coronal component detected in X-ray observations might then be coincident with the strongly magnetized flux tubes, or may be elsewhere. We note that for typical densities derived above, the hot and cool components will reach thermal equilibrium due to collisions on a timescale of order 10–20 s. The energy stored in the form of the hot coronal component for, e.g., YY Gem is 9×10^{32} ergs (using the numbers given above), and if this energy must continually be replenished as the hot plasma thermalizes the energy input required is of order 5×10^{31} ergs s^{-1}, which is much larger than the radiative energy-loss rate through X-ray emission, and is too large a fraction of the bolometric luminosity to be

believable. Thus it is clear that the hot and cool components cannot be cospatial. They are unlikely to be on the same field lines either; this would still require spatial separation of the two components with some form of "transition region" between them, given the rapidity of thermal conduction along magnetic field lines.

Note that pressure balance in the corona requires that loops with stronger magnetic field have less thermal material on them, so that $p + B^2/8\pi$ is balanced, but since (see § 3.3) the thermal energy density of the X-ray–emitting material is several orders of magnitude lower than the magnetic energy density this condition is not relevant to our problem.

2. The lower corona is indeed filled with strong magnetic fields as suggested earlier, but the hot X-ray–emitting component is not present in the low corona; rather it must be confined to the outer corona where the magnetic field strengths are lower. Nonetheless, the hot X-ray–emitting component must lie on closed field lines extending to a great height above the stellar surface. This is also the implication of the lack of observed eclipses of the hot component on RS CVn systems (White et al. 1986, 1990; Culhane et al. 1990). White et al. (1990) have suggested that the hot component of the X-ray–emitting plasma in those systems consists of the remnants of X-ray flares which have escaped from the original low-lying loops where the flare occurred and become trapped in closed loops much further out. The lifetime of the hot component due to radiative losses can be of the order of days.

This picture implies a fairly dynamic corona, with large flares producing ejections of very hot plasma which jostle their way out through closed loop systems up to a considerable height, expanding as they go until finally they rest at some height. The material trapped in these loops, if it maintains corotation with the star, must be traveling at several times the surface velocity. High-velocity cool material has in fact been seen in optical observations of AD Leo (Houdebine, Foing, & Rodonò 1990) and Gliese 890 (Doyle & Collier Cameron 1990). We note one difficulty with this picture: it is unlikely that the flare material itself is responsible for the loops ballooning out to great heights, because it would have to start off with a higher energy density than the magnetic fields which contain it in order to "blow" them open. If we continue to assume fields of 1 kG as typical in the low corona, the corresponding energy density is 4×10^4 ergs s^{-1}, and the number density of plasma at, say, 5×10^7 K required to match this energy density would be 4×10^{12} cm^{-3}. This is about an order of magnitude larger than is usually inferred for such flares on M dwarf flare stars (e.g., Linsky 1991). Thus a picture of flares occurring in simple loops which are then blown open by the pressure of the thermal material is not tenable. However, the large loops could be formed through reconnection of other overlying loops and realignment which allows loops originally "held in" to expand outward, as is thought to happen in solar filament eruptions.

The radiative cooling curve may be consistent with a picture in which the cooler component is due to a coronal heating mechanism and the hotter component is associated with cooling flare plasma which was initially very hot. The radiative cooling curve (e.g., Cox & Tucker 1969) shows a dip at $1–2 \times 10^7$ K, which can explain the presence of an observed component at 2×10^7 K since plasma which is initially much hotter than 2×10^7 K will cool quickly to that temperature and then cool much more slowly. However, there is no peak in the cooling curve at $6–9 \times 10^6$ K to explain the observed absence of coronal components in that temperature range; we must instead postulate that the cooler component is not due to cooling of hotter material, but rather to heating of initially cooler material.

We have not addressed the question of the location of the nonthermal radio-emitting electrons with respect to the hot component of the X-ray–emitting plasma. Since the nonthermal emission can vary by orders of magnitude from one day to the next, we do not require stable structures to contain the nonthermal electrons. Exceptions are cases like UV Ceti, which is always seen to have nonthermal emission at 5 GHz at about the same level. We can assume that the nonthermal emission we see at lower frequencies does not arise in the low corona where the magnetic fields are of kG strength, because the high implied brightness temperature of the nonthermal emission requires that it be produced by relatively high harmonics of the gyrofrequency, whereas if it were to come from the low corona it would be due to low harmonics (equivalently, the high magnetic fields render the corona optically thick at a high harmonic and prevent us from seeing down to the low corona). Thus the nonthermal electrons are also likely to be present at considerable heights above the stellar photosphere. They can quite happily coexist with the high-temperature thermal X-ray–emitting component, since their mutual collision frequency is low (Kundu et al. 1987).

6. CONCLUSIONS

We have shown that if the hot component of dMe-star coronae is confined to loops in the strong magnetic fields of the lower corona, it should be optically thick at 15 GHz and should produce radio fluxes which are easily detectable. Observations of a large sample of dMe stars do not show fluxes at the level implied at 15 GHz, and at 8 GHz the fluxes are often much larger than implied by the model. Consequently, these results indicate that the hot coronal component is not located in regions of strong magnetic field. The simplest explanation is that the hot component is largely confined to heights well above the low corona where the magnetic field strength exceeds 1 kG. X-ray eclipse observations may be able to confirm this conclusion; the same result has been argued to hold for RS CVn systems, based on eclipse observations. It is possible that the magnetic flux at the stellar photosphere does not reach the corona because it closes in the chromosphere, but this requires that the magnetic field be distributed as many oppositely polarized features several thousand kilometers across, which would be difficult to reconcile with the large photometric modulations attributed to spots.

If the coronae of these stars actually have a continuous distribution of emission measure and not a two-temperature structure, contrary to the fits of the IPC data by Schmitt et al. (1990), the problem will be exacerbated. This is because the radio opacity increases greatly with the energy of the electrons present, and a small number of nonthermal energetic electrons will produce much more flux than the corresponding lower energy thermal population.

The observations are consistent with a model in which the cooler coronal component is due to a magnetic solar-like coronal heating mechanism, while the hotter component is the remnant of hot flare plasma which has cooled to 2×10^7 K but cools only slowly beyond that temperature due to a dip in the radiative cooling curve. However, the spatial separation of the two components is not easy to explain. As on the Sun, it seems likely that stellar coronal flares occur in the low corona, among the loops containing the cool coronal component. The flare plasma must then move upward out of regions of strong

magnetic field; however, it is unlikely to have enough thermal energy density to overcome magnetic stresses, and thus can only propagate upwards if there is some rearrangement of magnetic fields associated with the flare which forces the plasma to move upward.

Research in stellar radiophysics at University of Maryland has been supported by NSF grants AST 91-14918 and 92-17891. Research at Caltech was supported by NSF grant ATM 90-13173. We thank the referee, S. Saar, for helpful discussions prior to the writing of the paper and for an excellent and thoughtful review. This research has made use of data obtained through the High-Energy Astrophysics Science Archive Research Center On-Line Service, provided by the NASA-Goddard Space Flight Center, and we thank S. Drake for some assistance.

REFERENCES

Agrawal, P. C., Rao, A. R., & Sreekantan, B. V. 1986, MNRAS, 219, 225
Bastian, T. S., & Bookbinder, J. 1987, Nature, 326, 678
Bastian, T. S., Bookbinder, J., Dulk, G. A., & Davis, M. 1990, ApJ, 353, 265
Bedford, D. K., Jeffries, R. D., Geyer, E. H., & Vilhu, O. 1990, MNRAS, 243, 557
Byrne, P. B. 1992, in Sunspots: Theory and Observations, ed. J. H. Thomas & N. O. Weiss (Dordrecht: Kluwer), 63
Cheng, C. C., & Pallavicini, R. 1992, Mem. Soc. Astron. Italiana, 63, 697
Choudhuri, A. R., & Gilman, P. A. 1987, ApJ, 316, 788
Cox, D. P., & Tucker, W. H. 1969, ApJ, 157, 1157
Cox, J. J., & Gibson, D. M. 1985, in Radio Stars, ed. R. M. Hjellming, & D. M. Gibson (Dordrecht: Reidel), 233
Cram, L. E., & Giampapa, M. S. 1987, ApJ, 323, 316
Culhane, J. L., White, N. E., Shafer, R. A., & Parmar, A. N. 1990, MNRAS, 243, 424
Donati, J., Brown, S. F., Semel, M., Rees, D. E., Dempsey, R. C., Matthews, J. M., Henry, G. W., & Hall, D. S. 1992a, A&A, 265, 682
Donati, J., Semel, M., & Rees, D. E. 1992b, A&A, 265, 669
Donati, J., Semel, M., Rees, D. E., Taylor, K., & Robinson, R. D. 1990, A&A, 232, L1
Doyle, J. G. 1987, MNRAS, 224, 1P
Doyle, J. G., & Collier Cameron, A. 1990, MNRAS, 244, 291
Fleming, T. A., Gioia, I. M., & Maccacaro, T. 1989, ApJ, 340, 1011
Gary, D. E. 1985, in Radio Stars, ed. R. M. Hjellming & D. M. Gibson (Dordrecht: Reidel), 185
———. 1986, in Cool Stars, Stellar Systems and the Sun, ed. M. Zeilik & D. M. Gibson (Berlin: Springer), 235
Gary, D. E., & Linsky, J. L. 1981, ApJ, 250, 284
Gary, D. E., Linsky, J. L., & Dulk, G. A. 1982, ApJ, 263, L79
Gliese, W., & Jahreiss, H. 1994, in preparation
Golub, L. 1983, in Activity in Red Dwarf Stars, ed. P. B. Byrne & M. Rodonò (Dordrecht: Reidel), 83
Güdel, M. 1992, A&A, 264, L31
———. 1993, in preparation
Güdel, M., & Benz, A. O. 1989, A&A, 211, L5
Haisch, B. M., Schmitt, J. H. M. M., Rodonò, M., & Gibson, D. M. 1990, A&A, 230, 419
Houdebine, E., Foing, B., & Rodonò, M. 1990, A&A, 238, 249
Jackson, P. D., Kundu, M. R., & White, S. M. 1987, ApJ, 316, L85
———. 1989, A&A, 210, 284
Katsova, M. M., Badalyan, O. G., & Livshits, M. A. 1987, Soviet Astron., 31(6), 652
Kundu, M. R., Jackson, P. D., White, S. M., & Melozzi, M. 1987, ApJ, 312, 822
Kundu, M. R., Pallavicini, R., White, S. M., & Jackson, P. D. 1988, A&A, 195, 159
Kundu, M. R., & Shevgaonkar, R. K. 1985, ApJ, 297, 644
———. 1988, ApJ, 334, 1001
Lacy, C. H. 1977, ApJS, 34, 479
Lang, K. R., & Willson, R. F. 1986, ApJ, 302, L17
———. 1988, ApJ, 326, 300
Lim, J., Nelson, G., & White, S. M. 1994, in preparation
Linsky, J. L. 1991, Mem. Soc. Astron. Ital., 62, 307
Linsky, J. L., & Gary, D. E. 1983, ApJ, 274, 776
Mathioudakis, M., Doyle, J. G., Rodonò, M., Gibson, D. M., Byrne, P. B., Avgoloupis, S., Linsky, J. L., Gary, D. E., Mavridis, L. N., & Varvoglis, P. 1991, A&A, 244, 155
Montesinos, B., & Jordan, C. 1993, MNRAS, in press
Nitta, N., et al. 1991, ApJ, 374, 374
Ottmann, R., Schmitt, J. H. M. M., & Kürster, M. 1993, ApJ, submitted
Pallavicini, R. 1992, in The Sun: A Laboratory for Astrophysics, ed. J. T. Schmelz & J. C. Brown (Dordrecht: Kluwer), 313
Pallavicini, R., Monsignori-Fossi, B. C., Landini, M., & Schmitt, J. H. M. M. 1988, A&A, 191, 109
Pallavicini, R., Tagliaferri, G., Pollock, A. M. T., Schmitt, J. H. M. M., & Rosso, C. 1990a, A&A, 227, 483
Pallavicini, R., Tagliaferri, G., & Stella, L. 1990b, A&A, 228, 403
Pettersen, B. R. 1980, A&A, 82, 53
———. 1991, Mem. Soc. Astron. It., 62, 217
Pollock, A. M. T., Tagliaferri, G., & Pallavicini, R. 1991, A&A, 241, 451
Rao, A. R., & Singh, K. P. 1990, ApJ, 352, 303
Robinson, R. D. 1980, ApJ, 239, 961
Rodonò, M., et al. 1989, in Solar and Stellar Flares, ed. B. M. Haisch & M. Rodonò (Catania: Catania Astrophysical Observatory), 53
Rucinski, S. M. 1985, MNRAS, 215, 591
Saar, S. H. 1988, ApJ, 324, 441
———. 1990, in Solar Photosphere: Structure, Convection and Magnetic Fields, ed. J. O. Stenflo (Dordrecht: Reidel), 427
———. 1992, in Proc. 7th Cambridge Workshop, Cool Stars, Stellar Systems and the Sun, ASP Conf. Ser., Vol. 26; ed. M. S. Giampapa & J. A. Bookbinder (San Francisco: ASP), 252
Saar, S. H. 1993, in IAU Symp. 154 Infrared Solar Physics, ed. D. Rabin & J. Jefferies (Dordrecht: Kluwer), in press
Saar, S. H., Piskunov, N. E., & Tuominen, I. 1992, in Proc. 7th Cambridge Workshop ,Cool Stars, Stellar Systems and the Sun, ASP Conf. Ser., Vol. 26, ed. M. S. Giampapa & J. A. Bookbinder (San Francisco: ASP), 255
Schmitt, J. H. M. M., Collura, A., Sciortino, S., Vaiana, G. S., Harnden, F. R., Jr., & Rosner, R. 1990, ApJ, 365, 704
Schmitt, J. H. M. M., Pallavicini, R., Monsignori-Fossi, B. C., & Harnden, F. R., Jr. 1987, A&A, 179, 193
Schüssler, M., & Solanki, S. K. 1992, A&A, 264, L13
Slee, O. B., Stewart, R. T., Nelson, G. J., Wright, A. E., Dulk, G. A., Bastian, T. S., & McKean, M. 1988, Astrophys. Lett. Comm., 27, 247
Solanki, S. K. 1992, in Proc. 7th Cambridge Workshop, Cool Stars, Stellar Systems and the Sun, ASP Conf. Ser., Vol. 26, ed. M. S. Giampapa & J. A. Bookbinder (San Francisco: ASP), 211
Stepień, K. 1988, ApJ, 335, 892
———. 1991, Acta Astron., 41, 1
Swank, J. H., & Johnson, H. M. 1982, ApJ, 259, L67
Topka, K., & Marsh, K. A. 1982, ApJ, 254, 641
Vogt, S. S. 1980, ApJ, 240, 567
Walter, F. M., Gibson, D. M., & Basri, G. S. 1983, ApJ, 267, 665
Webb, D. F., Holman, G. D., Davis, J. M., Kundu, M. R., & Shevgaonkar, R. K. 1987, ApJ, 315, 716
White, N. E., Culhane, J. L., Parmar, A. N., Kellett, B. J., Kahn, S., van den Oord, G. H. J., & Kuijpers, J. 1986, ApJ, 301, 262
White, N. E., Culhane, J. L., Parmar, A. N., & Sweeney, M. A. 1987, MNRAS, 227, 545
White, N. E., Shafer, R. A., Horne, K., Parmar, A. N., & Culhane, J. L. 1990, ApJ, 350, 776
White, S. M., Jackson, P. D., & Kundu, M. R. 1989, ApJS, 71, 895
White, S. M., Kundu, M. R., & Gopalswamy, N. 1992, ApJS, 78, 599
White, S. M., Kundu, M. R., & Jackson, P. D. 1986, ApJ, 311, 814
Zwaan, C., & Cram, L. E. 1989, in FGK Stars and T Tauri Stars, NASA SP 502, ed. L. E. Cram & L. V. Kuhi (Washington, DC: NASA/CNRS), 215